Climate Dynamics (2019) 52:6599–6617
https://doi.org/10.1007/s00382-018-4536-1

Indian summer monsoon onset forecast skill in the UK Met Office initialized coupled seasonal forecasting system (GloSea5-GC2)

Amulya Chevuturi[1,2] · Andrew G. Turner[1,2] · Steven J. Woolnough[1,2] · Gill M. Martin[3] · Craig MacLachlan[3]

Received: 24 May 2018 / Accepted: 12 November 2018 / Published online: 24 November 2018

Abstract

Accurate and precise forecasting of the Indian monsoon is important for the socio-economic security of India, with improvements in agriculture and associated sectors from prediction of the monsoon onset. In this study we establish the skill of the UK Met Office coupled initialized global seasonal forecasting system, GloSea5-GC2, in forecasting Indian monsoon onset. We build on previous work that has demonstrated the good skill of GloSea5 at forecasting interannual variations of the seasonal mean Indian monsoon using measures of large-scale circulation and local precipitation. We analyze the summer hindcasts from a set of three springtime start-dates in late April/early May for the 20-year hindcast period (1992–2011). The hindcast set features at least fifteen ensemble members for each year and is analyzed using five different objective monsoon indices. These indices are designed to examine large and local-scale measures of the monsoon circulation, hydrological changes, tropospheric temperature gradient, or rainfall for single value (area-averaged) or grid-point measures of the Indian monsoon onset. There is significant correlation between onset dates in the model and those found in reanalysis. Indices based on large-scale dynamic and thermodynamic indices are better at estimating monsoon onset in the model rather than local-scale dynamical and hydrological indices. This can be attributed to the model's better representation of large-scale dynamics compared to local-scale features. GloSea5 may not be able to predict the exact date of monsoon onset over India, but this study shows that the model has a good ability at predicting category-wise monsoon onset, using early, normal or late tercile categories. Using a grid-point local rainfall onset index, we note that the forecast skill is highest over parts of central India, the Gangetic plains, and parts of coastal India—all zones of extensive agriculture in India. El Niño Southern Oscillation (ENSO) forcing in the model improves the forecast skill of monsoon onset when using a large-scale circulation index, with late monsoon onset coinciding with El Niño conditions and early monsoon onset more common in La Niña years. The results of this study suggest that GloSea5's ensemble-mean forecast may be used for reliable Indian monsoon onset prediction a month in advance despite systematic model errors.

Keywords Indian summer monsoon · Monsoon onset · GloSea5-GC2 · Forecast skill · ENSO

1 Introduction

The Asian summer monsoon is a large-scale phenomenon directly impacting one third of the world's population with further influence on the global circulation. The monsoon over India, during the months of June, July, August and September (JJAS), provides approximately 80% of annual precipitation for the country. The precipitation brings respite from frequent heatwaves during the drier pre-monsoon season. Forecast of monsoon rainfall, its onset, advance and withdrawal are important for the rainfed agriculture sector. Prediction of the monsoon onset provides highly significant information for agricultural planning during the Kharif cropping season in July (Gadgil and RupaKumar 2006). Such

Electronic supplementary material The online version of this article (https://doi.org/10.1007/s00382-018-4536-1) contains supplementary material, which is available to authorized users.

✉ Amulya Chevuturi
a.chevuturi@reading.ac.uk

[1] National Centre for Atmospheric Science, University of Reading, Reading, UK

[2] Department of Meteorology, University of Reading, Reading, UK

[3] Met Office Hadley Centre, Exeter, UK

a forecast provides an indication of future water resource availability, which helps in planning strategies for sowing, transplanting and irrigation. Providing accurate and precise prediction of the monsoon onset can be very useful for developing the best agricultural strategies: to optimize utilization of favourable environmental conditions, the use of irrigation, and to mitigate severe impacts.

The months of extreme heat during the pre-monsoon lead to release of sensible heat flux from northern India and the Tibetan Plateau. This causes a large-scale reversal of the meridional temperature gradient at the surface and in the deep troposphere (Li and Yanai 1996), which is more than just land-ocean thermal contrast and is an important factor driving the deep baroclinic structure of the monsoon circulation (Xavier et al. 2007). The land-sea temperature contrast leads to a shallow circulation and convection (Schneider and Lindzen 1976). The deep tropospheric meridional temperature gradient leads to a strong pressure gradient causing the intense low-level cross-equatorial monsoon flow (Findlater 1969), providing the necessary moisture transport (Yanai et al. 1992; He et al. 2003; Xavier et al. 2007; Dai et al. 2013) along with the associated upper-level tropical easterly jet which leads to convective precipitation over the region (Koteswaram 1958). Thus, the Asian monsoon onset begins with surface heating over South Asia which leads to reduced near-surface layer stability, enhanced south-westerlies over the Bay of Bengal and south-easterlies over the South China Sea, and the development of Somali Jet and Iranian High. The monsoon onset is an abrupt phenomenon over the Indian landmass due to the sudden increase of kinetic energy (Raju et al. 2005).

The climatological monsoon onset over India is traditionally considered as 1 June with a standard deviation of 7 days, with monsoon precipitation covering whole of India by mid-July (Krishnamurthy and Shukla 2000). The continental Indian summer monsoon onset begins along the coast of Kerala (Ananthakrishnan and Soman 1988). After the initial onset, further advance of the monsoon occurs from south to northwest in a direction that is perpendicular to the monsoon flow due to the presence of mid-level north-westerly dry winds which are slowly overcome by low-level moist flow from the tropics (Parker et al. 2016). The monsoon begins its withdrawal in September, which is more gradual than the onset.

The India Meteorological Department (IMD) used to operationally declare the monsoon onset over Kerala (MOK) through estimates of rainfall over meteorological stations in Kerala (Ananthakrishnan and Soman 1988; Soman and Kumar 1993). However, due to the subjective nature of this method, there might be inconsistencies in the case of bogus onsets, as it occurred for example in 2002 (Flatau et al. 2003). From 2006 onwards, IMD started using monsoon onset criteria from Joseph et al. (2006) and Pai and Rajeevan (2009) based on rainfall over 14 stations in Kerala, zonal wind over 5°–10°N and 70°–80°E, and outgoing longwave radiation (OLR) over 5°–10°N and 70°–75°E. IMD finally determines and reports reanalyzed monsoon onset dates based on instrumental rainfall.

Different studies have used understanding of dynamic and thermodynamic characteristics of the monsoon to develop various objective criteria to define monsoon onset indices. The studies have suggested indices based on: temperature changes (Ramesh et al. 1996; Prasad and Hayashi 2005; Goswami and Xavier 2005; Goswami et al. 2006; Xavier et al. 2007), strengthening of wind shear over Asia (Webster and Yang 1992; Goswami et al. 1999), enhanced low-level circulation (Wang and Fan 1999; Wang et al. 2009, 2001; Taniguchi and Koike 2006), hydrological features such as atmospheric moisture content (Goswami et al. 1999; Fasullo and Webster 2003; Zeng and Lu 2004) and combinations of multiple variables such as wind and OLR (Joseph et al. 2006; Pai and Rajeevan 2009). Aside from the above indices, which define a single onset date in each case for the whole country in each year, some studies also proposed spatially varying local monsoon onset indices based on precipitation patterns (Wang and LinHo 2002; Moron and Robertson 2014). The limitation of using large-scale indices compared to local indices is that they might ignore the synoptic-scale forcing of monsoon variability. However, Pai and Rajeevan (2009) showed potential predictability of the monsoon onset using large-scale features of the monsoon.

Interannual variability of the Indian monsoon onset might be affected by teleconnections from the El Niño Southern Oscillation (ENSO; Webster and Yang 1992; Goswami and Xavier 2005; Turner et al. 2005; Roy et al. 2016). Observational studies suggest that El Niño years may lead to a late monsoon onset over India whereas La Niña conditions may cause early onsets (Joseph et al. 1994; Xavier et al. 2007; Lau and Nath 2012; Adamson and Nash 2014). Many studies have detailed the influence of ENSO on different monsoon onset indices using observed data (Webster and Yang 1992; Wang and Fan 1999; Xavier et al. 2007).

Alessandri et al. (2015) show good forecasting skill of the monsoon onset in the Centro Euro-Mediterraneo sui Cambiamenti Climatici Climate (CMCC) sub-seasonal prediction system when the atmosphere is initialized from reanalysis. With only very few studies analyzing the forecast skill of Indian monsoon onset in different models, there is a need to understand the ability of initialized coupled models at predicting monsoon onset in greater detail, and in a wider range of models. Further, due to the importance of the Indian monsoon onset date for end-users, there is value in quantifying GloSea5's skill at forecasting the large-scale and local monsoon onset and its relationship with ENSO forcing.

GloSea5, similar to other contemporary initialized coupled models, shows modest skill at predicting Indian

monsoon rainfall, but has much higher skill at predicting large-scale circulation (Johnson et al. 2017). ENSO forcing is a potential source of predictability of the ISM in GloSea5 due to its known impact on ISM rainfall, which may improve forecast skill during the years with ENSO forcing (Johnson et al. 2017). Climatological dynamic and thermodynamic physical processes are well represented in GloSea5 seasonal hindcasts during the monsoon onset (Menon et al. 2018). Building upon the work of these two papers, we assess and demonstrate the skill of the GloSea5 initialized coupled seasonal prediction system in forecasting the Indian monsoon onset. To present a well-rounded assessment of skill, we use five objective onset indices based on different physical aspects of the monsoon onset (instead of the classical subjective criterion of increased rainfall over a small region of Kerala) to estimate onset dates in the model and reanalysis data. GloSea5 onset dates are verified exhaustively against the reanalyses to quantify the monsoon onset forecasting skill in GloSea5. We further analyze the influence of ENSO forcing on the forecast skill. The results of this study provide evidence supporting the use of GloSea5 as a forecasting tool for operational prediction of the Indian summer monsoon onset.

In Sect. 2, we provide a detailed description of the forecast system, data analyzed, indices used to estimate monsoon onset and our methodology for estimating the model's forecast skill. The performance and skill of the GloSea5 model at predicting the monsoon onset date are described in the next two sections; Sect. 3 discusses the model's ability to capture the onset dates in different years and Sect. 4 analyzes the model skill at predicting the tercile categories of monsoon onset and the impact of large-scale ENSO forcing on onset prediction skill. We summarize and conclude our study in Sect. 5.

2 Methodology

2.1 Data

2.1.1 Model data

In this study, we analyze the Met Office Global Seasonal Forecast version 5 (GloSea5) hindcast dataset. GloSea5 in Global Coupled configuration 2 (GC2) (Williams et al. 2015) has components as summarized in Table S1. It is a seamless monthly/seasonal forecast system used for operational forecasting (MacLachlan et al. 2015). For our study, focus is on analysis of a 20-year research hindcast set, which differs from the operational seasonal forecast only in its atmosphere initialization (see Table S1). The hindcasts cover the years 1992–2011, and the relevant outputs covering the Indian summer monsoon season (June–August) are initialized on three start-dates each year: 25 April (hereafter 0425), 1 May (hereafter 0501) and 9 May (hereafter 0509). Each seasonal hindcast is integrated for 140 days, with eight members for each start-date for 1992–1995 and 2010–2011 and five members each for 1996–2009. The spread in ensemble initial conditions for each year (≈15 members per year) is generated using a stochastic physics scheme SKEB2 (Bowler et al. 2009).

2.1.2 Observed data

The European Centre for Medium-range Weather Forecasts (ECMWF) Interim Reanalysis, known as ERA-Interim (Dee et al. 2011) has been used for comparison with the model output for dynamic and thermodynamic fields. We used daily mean data for the zonal component of wind, specific humidity and temperature at different pressure levels.

For rainfall observations we used the GPCP dataset (Global Precipitation Climatology Project; Adler et al. 2003). The various observed gridded rainfall products covering India have a range of pros and cons when assessed using a range of skill metrics (Prakash et al. 2015). A common error is their poor simulation of orographic rainfall. However, here we use GPCP due to its better representation of the Indian monsoon in comparison to other merged rainfall datasets (Prakash et al. 2015).

2.2 Analysis methods

2.2.1 Identifying monsoon onset

Identifying the monsoon onset in models is a challenge. IMD declares the Indian monsoon onset as rainfall over Kerala (MOK; refer to Sect. 1). This methodology cannot be used to determine onset using reanalysis data due to the coarse resolution, and cannot be used with model output since most models do not forecast local-scale features very well. Instead objective monsoon onset indices can be used, which reflect the key physical mechanisms associated with the monsoon. These provide a single onset date for the large-scale monsoon and its interannual variability, while being resistant to local processes, bogus onsets and synoptic disturbances (Flatau et al. 2001; Fasullo and Webster 2003). These indices are usually based on a monsoon onset trigger mechanism (circulation, temperature, rainfall and moisture) and must have a relatively large spatial scale, for which most models are able to capture the interannual variability fairly well (Fasullo and Webster 2003; Alessandri et al. 2015).

After reviewing a range of monsoon onset indices, we note that no single index is based on all physical aspects of the monsoon onset. Hence, in this study we compare five different monsoon onset indices (Table 1) to analyze the performance of the model. Four of the indices provide a

Table 1 Details of monsoon onset indices used in this study

Index	Methodology	Onset	Reference	Region
Tropospheric Temperature Gradient Index (TTGI)	TTGI = T_N - T_S T = Vertically averaged temperature (600 - 200 hPa) T_N = T(40°-100°E, 5°-35°N) T_S = T(40°-100°E, 15°S-5°N)	Onset defined when TTGI time-series for each year becomes positive	Xavier et al. (2007)	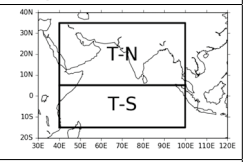
Webster and Yang Index (WYI)	WYI = U_{850} - U_{200} U = Zonal Wind at 850 or 200 hPa U = U(40°-110°E, 0°-20°N)	Onset defined when seven-day running average of WYI time-series crosses threshold value (mean ERA-Interim value on climatological onset, 30May)	Webster and Yang (1992)	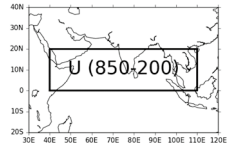
Hydrological Onset and Withdrawal Index (HOWI)	HOWI = nVIMT(1000 - 300 hPa) nVIMT = Vertically integrated zonal moisture transport (300-1000hPa) normalized over the annual cycle nVIMT = nVIMT(45°-80°E, 5°-20°N)	Onset defined when HOWI time-series for each year becomes positive	Fasullo and Webster (2003)	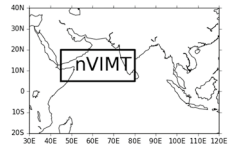
Wang and Fan Index (WFI)	WFI = U_S - U_N U = Zonal Wind at 850 hPa U_S = U(40°-80°E, 5°-15°N) U_N = U(70°-90°E, 20°-30°N)	Onset defined when seven-day running average of WFI time-series becomes positive	Wang and Fan (1999)	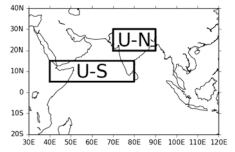
Wang and LinHo Index (WLI)	WLI = P - Rjan P = Pentad rainfall for different years Rjan = Mean rainfall for Jan of respective years	Onset on pentad when the five-pentad running average of WLI time-series for each grid-point for each year crosses the threshold of 5 mm/day^{-1}	Wang and LinHo (2002)	Spatial Variability

single large-scale onset date for the Indian monsoon. The fifth index provides local monsoon onset dates at each grid-point as the monsoon progresses over India. The five different indices used in the study are based on specific changes associated with monsoon onset: (a) meridional tropospheric temperature gradient, (b) zonal wind-shear change, (c) moisture convergence (moisture and circulation), (d) low-level wind circulation, and (e) local rainfall increase. In our study, the monsoon onset date with each index is defined using a threshold criterion based on absolute index values. This method can be considered as a rigorous test for a model's capacity to accurately represent the monsoon onset. Detailed descriptions of the indices are given below, starting at the largest scale and working towards grid-point local precipitation.

(A) *Tropospheric temperature gradient index (TTGI)*

Xavier et al. (2007) proposed a monsoon onset index based on large-scale thermodynamic forcing of the monsoon, TTGI. Springtime warming over the Asian region and an elevated heat pump due to the Tibetan Plateau lead to the establishment of a meridional temperature gradient in the upper troposphere over the region. This temperature gradient is shown to drive the moisture-laden cross-equatorial flow leading to monsoon onset. TTGI is defined as the difference between vertically averaged tropospheric temperature over 600–200 hPa between a northern box (T_N) and southern box (T_S) demarcated in Table 1. In ERA-Interim by design, atmospheric hybrid pressure levels intersecting orography (such as over the Himalaya and Tibetan Plateau) are interpolated from the lowest pressure level above the surface. In model output, such levels are assigned missing values. Thus to avoid discrepancy, we overwrite ERA-Interim values at grid-points below steep orography with missing data as determined using the model orography.

The onset is defined using TTGI when its sign changes from negative to positive (Xavier et al. 2007), meaning a threshold of 0 K marks the onset date. When TTGI is positive, it represents the northern region being warmer than the south. To clearly show how the monsoon onset date is defined in our study from the TTGI in the model and ERA-Interim, we show an example in Fig. 1a. Figure 1a shows the range of TTGI seasonal cycles in 0501 start date ensemble members (red; 0501_ALL-ENS_1992-2011) and ERA-Interim (grey; ERA_1992-2011) for all of the 20 years. The upper and lower terciles (for the whole inter-annual spread) at which the TTGI crosses the zero-threshold are marked as vertical dashes. We use these vertical dashes to define whether a given ensemble member for a particular year features a late or early onset compared to the overall distribution for the model (and likewise for ERA-Interim).

To clarify the calculation of monsoon onset date and its categorization as early/normal/late onset we show (Fig. 1a) an example year of 1992 as solid lines for one ensemble

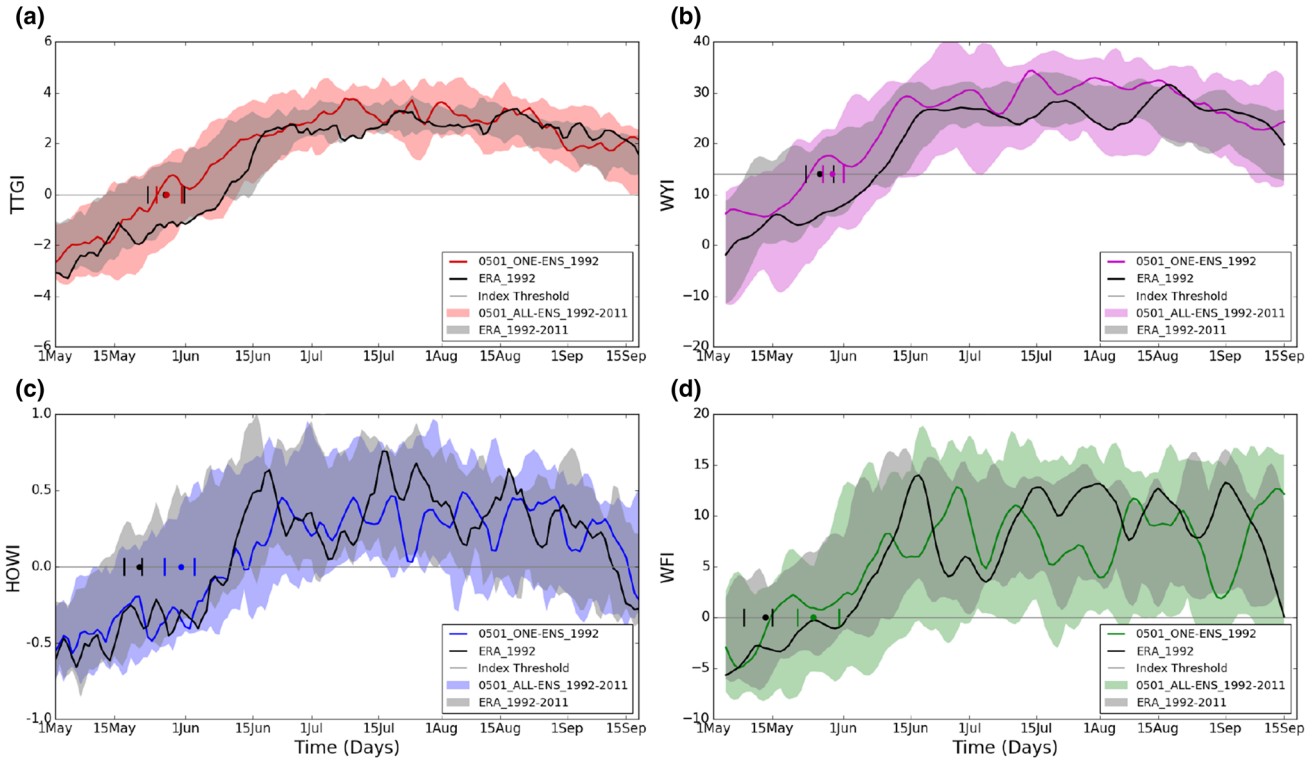

Fig. 1 Climatological daily evolution of monsoon onset indices in ERA-Interim reanalysis and the 0501 start-date ensemble-members of GloSea5. For illustration we also show 1992 as an example year in each case. Onset indices shown are **a** TTGI (red), **b** WYI (magenta), **c** HOWI (blue) and **d** WFI (green) as defined in Table 1. The color and grey shaded regions show the interannual spread of the monsoon onset index with all ensemble members of 0501 and ERA-Interim respectively from 1992–2011. The solid lines represents 1992, as an example year within the interannual spread, for ERA-Interim (black, ERA_1992) and one random ensemble member for 0501 (colored, 0501_ONE-ENS_1992). The grey horizontal line is the chosen threshold for each index, where monsoon onset is defined as the date when the daily time series crosses the threshold. The small vertical dashes represent the lower and upper terciles (indicating early and late onset bounds) and dots represent each index's mean monsoon onset for 0501 (colored) and ERA-Interim (black)

member of 0501 (red; 0501_ONE-ENS_1992) compared to ERA-Interim (black; ERA_1992). The TTGI monsoon onset date for 1992 is defined when the solid lines cross the zero-threshold (Index Threshold). The TTGI monsoon onset date for 1992 for that ensemble member of 0501 is 25 May or 11 Jun in ERA-Interim. As the onset date for ERA-Interim is later than the upper tercile of the interannual spread we assign this year as late onset for ERA-Interim with TTGI. But 1992 is assigned as a normal onset year for this ensemble member of 0501 in the model, as the onset date lies between the upper and lower tercile lines.

(B) *Webster and Yang index (WYI)*

Webster and Yang (1992) described the strengthening of the lower tropospheric westerlies and upper tropospheric easterlies during the monsoon period over South Asia. The low-level westerly flow arises from the Coriolis force acting on the cross-equatorial component of the monsoon Hadley Circulation. The upper-level tropical easterly jet over India originates from the thermal wind balance of the temperature gradient between the warm troposphere over the Tibetan Plateau and relatively cooler troposphere over the Indian Ocean. This variation in the vertical wind shear captures the interannual variability of the Indian summer monsoon quite well. Thus, the Webster and Yang circulation index (WYI) considers the contrast between zonal winds at lower levels (850 hPa) and in the upper troposphere (200 hPa) over the large-scale South Asian region demarcated by the box in Table 1. Webster and Yang (1992) did not explicitly define a threshold for monsoon onset using the WYI but show that large-scale strengthening of the vertical windshear starts at the monsoon onset and is associated with decreasing OLR, representing convective heating. Johnson et al. (2017) showed that GloSea5 has good skill predicting the seasonal-mean WYI with a correlation score against ERA-Interim of 0.6. In this study we further examine the model's skill at predicting Indian monsoon onset using WYI.

The seasonal cycle of WYI is depicted in Fig. 1b for 0501 (magenta) and ERA-Interim (black) with the interannual spread (shaded) and one ensemble member for 1992 (solid line). Due to the noisy nature of circulation time

series and to prevent assigning bogus onsets, we smooth the WYI time series of both model and ERA-Interim using a seven-day moving average (7-Av). Next, we use the climatological value of ERA-Interim WYI index on 30 May as our threshold for WYI (as 30 May is the mean climatological onset date for 1992-2001 for IMD issued monsoon onset dates). This is also done by Alessandri et al. (2015) who used this method for defining monsoon onset for another circulation index described by Wang et al. (2009). Thus, the threshold used for defining WYI onset date is when the 7-Av seasonal time series of WYI crosses 14.08 m s^{-1} (grey horizontal line in Fig. 1b).

In Fig. 1b, the interannual spread of 7-Av WYI in ERA-Interim (grey) and 0501 ensemble members (magenta) is shown together with the 1992 example year. The date on which the lines cross the threshold (14.08 m s^{-1}), is defined as the onset date for the ensemble member of 0501 (23 May) and ERA-Interim (10 Jun). Since the onset date for 0501 ensemble member in 1992 is before the lower tercile it will be categorized as an early onset, whereas it will be considered a late onset for ERA-Interim for 1992 as it falls after the upper tercile date.

(C) *Hydrological onset and withdrawl index (HOWI)*

Fasullo and Webster (2003) argued that the monsoon is best identified by the hydrological processes involved. The horizontal moisture convergence over the Bay of Bengal and Southeast Asia (where precipitation exceeds evaporation) is in contrast with moisture source regions identified by moisture divergence, such as the Arabian Sea and Southern Hemisphere Indian Ocean. They used vertically integrated moisture transport (VIMT) as an indicator of monsoon hydrology and circulation. VIMT is the product of specific humidity and zonal wind, vertically integrated over 1000–300 hPa. The VIMT is normalized (nVIMT) over the annual cycle and calculated as in the equation below:

$$nVIMT = 2 \times \frac{VIMT - min(VIMT)}{max(VIMT) - min(VIMT)} - 1 \quad (1)$$

where max(VIMT) and min(VIMT) represent the maximum and minimum VIMT, respectively, over the whole time period of study. As described in Table 1, the HOWI index is averaged over a region encompassing the Arabian Sea, an important moisture source for the Indian monsoon (e.g. Levine and Turner 2012).

The annual cycle of HOWI becomes positive as the monsoon sets in (Fasullo and Webster 2003). Thus, zero is considered as the threshold for defining the onset date for HOWI. In Fig. 1c, the date on which the lines cross the threshold (0) is 13 Jun for both this example ensemble member of 0501 and ERA-Interim for 1992. As both these dates fall after the upper tercile dates for both 0501 and ERA-Interim, we would consider these as late onsets.

(D) *Wang and Fan index (WFI)*

Wang and Fan (1999); Wang et al. (2009) found that the 850 hPa vorticity has a good correlation with the rainfall. But as the zonal winds dominate the vorticity rather than meridional winds, they used the 850 hPa zonal winds for their index (Wang et al. 2001). The tropical monsoon westerlies over the Arabian Sea are in contrast to the easterly flow typically experienced further north adjacent to the Himalayas. Thus, the Wang and Fan Index (WFI), is the difference between the 850 hPa zonal wind over the two regions U_N and U_S demarcated in Table 1.

According to Wang et al. (2001), the temporal evolution of the WFI is enhanced by the strong low-level westerlies during the monsoon onset, the changing sign from negative to positive indicating the onset date (Syroka and Toumi 2004). As in the case of WYI, a 7-Av WFI time series is considered for analysis rather than the raw time series, which was noisy. Figure 1d shows that the onset date on which the lines cross the threshold (0 m s^{-1}) is 13 Jun for the example ensemble member of 0501 in 1992 and 2 Jun for ERA-Interim in 1992. Since the onset date for the 0501 ensemble member in 1992 is before the lower tercile it will be categorized as an early onset. Whereas it will be considered a late onset for ERA-Interim in 1992 as it falls after the upper tercile date.

(E) *Wang and LinHo index (WLI)*

The above four monsoon onset indices provide single monsoon onset dates for India for each year, irrespective of locality. However, information on the local monsoon onset is invaluable for strategic planning in agriculture, for example to decide sowing times etc. Thus, we also need a monsoon onset index that shows spatial variability of the ISM onset. In this study we use the monsoon onset index of Wang and LinHo (2002), hereafter WLI, which is one of the few indices providing variability at local spatial scales. Wang and LinHo (2002) proposed that monsoon onset should be defined in terms of rainfall characteristics relative to the minimum in the annual cycle. To avoid noise inherent in rainfall time series, the WLI spatial monsoon onset index is calculated using smoothed pentad rainfall time series (P). The climatological January-mean rainfall is subtracted from the pentad precipitation time series throughout the year in order to distinguish the monsoon regime from the winter dry season. We obtain the climatological January-mean rainfall from GloSea5 hindcasts performed for the DJF season, initialized in December. The monsoon onset pentad for each grid-point is determined as the time when the five-pentad

running average of relative rainfall exceeds 5 mm day^{-1} (Table 1). Though this index has previously been used to assess monsoon onset in climatological data, we have used it here for analyzing the local monsoon onset of each individual year and for each ensemble member. Using the five-pentad running average for relative rainfall (Sperber et al. 2013) on each start date ensemble member for each year smooths the rainfall time series sufficiently to reduce its sensitivity to noise.

Similarly, using the above methodology we calculate monsoon onset dates for each year from 1992–2011 for all four indices for all model ensemble members and ERA-Interim. Then using the onset dates for each ensemble member we calculate the mean onset dates for all start-date ensembles (denoted as 0425_MN, 0501_MN and 0509_MN) for each year. We also calculate the model grand ensemble onset mean (denoted by MOD_MN) by averaging onset dates for all ensemble members for all start date initializations for each year. Further, we also designate early/normal/late onset years using different indices for all years and all ensemble members, as in our example year of 1992.

2.2.2 Measures of model skill

As described in the example figure (Fig. 1), each onset index is calculated for reanalyses (ERA-Interim) and GloSea5. For this study we calculate all the model ensemble members onset dates for each year (0425_ENS, 0501_ENS and 0509_ENS), the mean onset date for each start-date for each year (0425_MN, 0501_MN and 0509_MN) and the model grand ensemble onset mean (MOD_MN). The model means are calculated as the mean onset date between all their respective model initializations' ensemble member onsets for each year. The model performance in forecasting the monsoon onset date with each index is compared with the ERA-Interim reanalysis onset date using the same index.

Comparison of interannual variability between hindcast and observed monsoon onset dates is done using the Pearson correlation coefficient. Further, the significance of the correlation coefficient is tested using the Student's t test, where a p value of less than 0.05 shows a 95% confidence level in the correlation coefficient. However, the presence of a correlation does not always imply predictability. We therefore also estimate the potential predictability in GloSea5 using the ratio of predictable component (RPC; Eade et al. 2014).

$$RPC = \frac{r}{\sqrt{\sigma^2_{sig}/\sigma^2_{tot}}} \tag{2}$$

where r is the correlation coefficient between GloSea5 and reanalysis, σ^2_{sig} is the signal variance of the model ensemble mean and σ^2_{tot} is the variance of all ensemble members. A forecasting system having RPC equal to 1 reflects the maximum potential predictability.

The skill of GloSea5 at forecasting the monsoon onset for each of the indices has been further quantified using different skill-scores applied to tercile categories of monsoon onset (early, normal and late). GloSea5 does not capture the exact monsoon onset date for each year when compared against ERA-Interim, but it may capture the interannual variability of the onset dates when considering onset categories for the interannual spread divided into terciles. So the model skill in the study is calculated as scores on the basis of model onset prediction of the onset category compared against reanalysis. The skill-scores used in this study can be divided into two categories depending on whether they are calculated for mean onset dates (for each start-date ensemble mean, 0425_MN, 0501_MN, 0509_MN, and MOD_MN) or from the individual ensemble members of each start-date (0425_ENS, 0501_ENS, 0509_ENS) and the set of all model ensemble members (MOD_ENS), as described below. Each skill score's forecast verification strengths are described on the basis of the attributes of Murphy (1993).

(A) *Model-ensemble mean skill-scores*

For a 20-year onset date time series whether start-date ensemble mean or MOD_MN (deterministic forecasts), onset forecast skill-scores are calculated using Accuracy, ACC, and Heidke skill-score, HSS (IRI 2013; WCRP 2015).

ACC is a score that defines the accuracy of the model performance.

$$ACC = \frac{1}{N}\sum_{i=1}^{C} n(F_i, O_i) \tag{3}$$

where C is the different category of forecast (early/normal/late), N is the total number of forecasts (years) and $n(F_i, O_i)$ is the accurate number of forecasts for all the different categories over the years. It quantifies the fraction of forecasts predicting the correct tercile category amongst all forecasts and ranges from 0 (no skill) to 1 (perfect score).

HSS is defined as the accuracy of forecasts at predicting the category, relative to that of random chance; e.g., under random circumstances, we would predict the model to forecast a late onset one third of the time.

$$HSS = \frac{\frac{1}{N}\sum_{i=1}^{C} n(F_i, O_i) - \frac{1}{N^2}\sum_{i=1}^{C} n(F_i)n(O_i)}{1 - \frac{1}{N^2}\sum_{i=1}^{C} n(F_i)n(O_i)} \tag{4}$$

where C is the number of forecast categories, N is the total number of forecasts, $n(F_i, O_i)$ represents the accurate forecasts and $n(F_i)n(O_i)$ is all the combinations of expected forecast and observed category combinations. This score ranges

from $-\infty$ to 1, with 0 meaning no skill and 1 meaning a perfect forecast score for the model. Negative values for HSS indicate that the model forecast is worse than a randomly generated forecast set. HSS represents forecast quality on the basis of discrimination, reliability and resolution.

(B) *Model-ensemble skill-scores*

In order to validate the performance of GloSea5 in representing monsoon onset, it is imperative that we do not just analyze mean monsoon onset, but we must also understand the performance of individual model ensemble members. For analysing the onset forecast skill of each member for each start-date, we calculate 'probabilistic forecasts' for the three onset categories (early, normal and late). For example, probabilistic forecasts of an early onset for each model start-date are calculated as the number of model ensemble members forecasting an early onset divided by the total number of ensemble member forecasts. Probabilistic forecasts for each start date for the three categories are verified against ERA-Interim onset tercile category using Brier Skill Score, BSS, and Ranked Probability Skill Score, RPSS (IRI 2013; WCRP 2015).

BSS defines the magnitude of the Probabilistic forecast errors of each category and measures the mean-squared forecast probability error. To account for the small ensemble size of our dataset, we use discrete BSS (dBSS), using an extra correction term "D" (Weigel et al. 2007), which will be detailed at the end of this section.

$$dBSS = 1 - \frac{BS_c}{BS_{clim} + D} \tag{5}$$

where BS_c is the Brier Score of a particular category which is calculated as follows:

$$BS_c = \frac{1}{N}\sum_{i=1}^{N}(F_i - O_i)^2 \tag{6}$$

where F is the forecast probability of that category, O is the observed category and N_c is the number of forecasts in the same category. O is 1 for the observed category and 0 for other categories.

BS_{clim} is the reference BS climatology, calculated with the same formula as BS_c but with climatological probability of 1/3 for the value of F in all the cases. dBSS ranges from $-\infty$ (highest possible error) to 1 (perfect score), with 0 indicating no skill when compared to BS_{clim}. This score is calculated for all three onset categories. dBSS reflects the mean-squared probability error, which represents reliability, resolution and uncertainty in forecasts.

RPSS measures the sum of squared probability errors, which is cumulative across the three forecast categories in order from early to normal to late onsets.

$$dRPSS = 1 - \frac{RPS}{RPS_{clim} + D} \tag{7}$$

where RPS is the Ranked probability Score which is calculated as follows:

$$RPS = \frac{1}{N}\sum_{i=1}^{N}\left[\frac{1}{(C-1)}\left(\sum_{j=1}^{C}(F_j - O_j)^2\right)\right] \tag{8}$$

where F is the forecast probability, O is the observed category, N is the number of forecasts and C is the number of forecast categories (1) early, (2) normal, (3) late; quantified as cumulative categorical forecast probability in the given order. RPS_{clim} is the reference RPS climatology, calculated with the same formula as RPS, but with climatological probability of 1/3 for the value of F in all the cases. dRPSS defines how well the probabilistic forecast predicts the actual observed category and ranges from $-\infty$ (highest possible error) to 1 (perfect score), with 0 indicating no skill when compared to RPS_{clim}. dRPSS indicates the forecast errors due to systematic biases and represents attributes of discrimination, reliability and resolution.

The correction term "D", in both dRPSS and dBSS, is indirectly proportional to the ensemble members and is negligible for large ensemble sizes.

$$D = \frac{1}{M}\sum_{i=1}^{K}\left[p_i\left(1 - p_i - 2\times\sum_{j=i+1}^{K}p_j\right)\right] \tag{9}$$

where M is the ensemble size and p is the reference forecast probability climatology at each forecast categories K. D is calculated as the mean over all years to account for the variable ensemble members in our model dataset. Weigel et al. (2007) suggested that there should be a clear impact of the correction term on the skill score due to the small ensemble size and low differences between the probabilities of the forecast categories.

2.2.3 ENSO forcing

For understanding the influence of ENSO on predictability of the Indian monsoon onset, we use two different methods. These methods analyze any influence of ENSO forcing on monsoon onset forecast skill and the predisposition of early or late monsoon onset influenced by El Niño or La Niña conditions.

In the first method, we consider the years which are either El Niño or La Niña years (known collectively as ENSO years) during our 20-year period of the start date

means. The coupled hindcast model may develop ENSO conditions during the summer from signals of anomalous heat content already present above the equatorial Pacific thermocline in the initial state. We designate a year as an ENSO year using the Ocean Niño Index (ONI). If the model SST anomalies for June to August averaged over the Niño-3.4 region (5°N–5°S, 160°E–150°W) exceed 0.5 °C or are below − 0.5 °C then we define it as an ENSO year otherwise it is considered an ENSO-Neutral year. Thus, out of 20 years (1992–2011) we have 11 ENSO years in the model (1992, 1993, 1995, 1997, 1998, 1999, 2000, 2003, 2007, 2009 and 2010), which will be referred to as ENSO11.

In order to understand whether the forecast skill improves during ENSO11 years, we will compare the skill of the ensemble-mean onset dates for those 11 years with the skill of the ensemble-mean onset dates for the full 20 year dataset, using ACC and HSS. However, performing straightforward comparisons will not allow assessment of statistical significance due to the small sample size. Thus, in order to interpret any impact of ENSO forcing on onset forecast skill and rule out making erroneous findings due to chance, we calculate skill-scores for randomly sampled 11-year periods from the 20 year dataset of ensemble-mean onset dates, with no replacement in each sample. This random sampling is repeated 10,000 times to get a distribution of skill-scores for 11-year collections of start date means (0425_MN, 0501_MN, 0509_MN and MOD_MN) and this distribution will be referred to as RANDOM11. We assume that, given the large number of random samples, our distribution will be representative of skill-score range (ACC and HSS) for 11-year samples. By analyzing the position of the ENSO11 collection of model ensemble means within the respective RANDOM11 distribution, we can diagnose the influence of ENSO on monsoon onset forecast skill with statistical confidence.

In the second method we determine El Niño, La Niña and ENSO-Neutral years and the onset categories for each individual ensemble member. Instead of categorizing the ENSO years depending on a threshold, we determine the ENSO categories (El Niño, La Niña and neutral) based on tercile categories of the ONI index. Thus, in this case we designate a year as El Niño when the ONI index is greater than the upper tercile of the model mean ONI spread, La Niña when ONI is lower than the lower tercile and the remaining years are designated as neutral. Consideration of each individual ENSO category (El Niño, La Niña or neutral) in concurrence with one of the three monsoon onset categories (early, normal and late) leads to nine possible combinations. We calculate the frequency of occurrence of each of the nine combinations for all 20 years. Higher frequency of certain combinations might indicate a connection between that particular forcing and the occurrence of that monsoon onset category.

3 Monsoon onset interannual variability

In this section we examine the model performance at predicting the monsoon onset using the five different indices (TTGI, WYI, HOWI, WFI and WLI as described in Sect. 2.2.1). Monsoon onset dates calculated with the four area-averaged indices are shown in Fig. 2, for all model ensemble members (0425_ENS, 0501_ENS, 0509_ENS, MOD_ENS), ensemble-means (0425_MN, 0501_MN, 0509_MN, MOD_MN) and reanalysis, and also as a cumulative distribution function in Fig. S1. In all the panels of Fig. 2, the box plots show the ensemble member spread of onset dates for each initialization (0425-blue, 0501-red and 0509-green) for all years. The mean monsoon onset date and interannual standard deviation of the whole ensemble are presented in Table 2.

3.1 TTGI

The mean onset date with TTGI for MOD_ENS is 28 May and for ERA-Interim is 27 May (Table 2). The mean monsoon onset with TTGI in GloSea5 shows a delay by only one day compared to the ERA-Interim mean monsoon onset date. Contemporary studies (Xavier et al. 2007; Saha et al. 2014; Senan et al. 2016) using different observational datasets also show similar mean monsoon onset dates for TTGI: NCEP (1950–2003) 30 May, ERA-Interim (1989–2009) 28 May, NCEP (1979–2009) 1 Jun, ERA-Interim (1980–2009) 29 May, respectively. According to Prodhomme et al. (2015), the SINTEX-F2 coupled model shows a delayed mean monsoon onset compared to ERA-Interim using TTGI, due to atmosphere-ocean coupling or SST errors in the coupled version, whereas the atmosphere only version simulated the monsoon onset earlier than ERA-Interim.

The interannual variability of the TTGI monsoon onset in GloSea5 MOD_ENS features a similar standard deviation (7 days) to that of the observational datasets in this or other studies (7–8 days; Xavier et al. 2007; Saha et al. 2014; Senan et al. 2016).

The GloSea5 monsoon onset forecast skill using TTGI is good, as seen from the significant correlation between MOD_MN and ERA-Interim (0.9) for 1992–2011 (Table 3). ECMWF System 4 seasonal hindcast set (1981–2010) of early April initialization, has a correlation of 0.77 with ERA-Interim (Senan et al. 2016). The RPC of GloSea5 with TTGI is close to or slightly higher than 1 for all start dates (Table 4), suggesting slightly underconfident forecasts. This suggests a low signal-to-noise ratio or a high correlation between ensemble member means with observations but low inter-ensemble agreement.

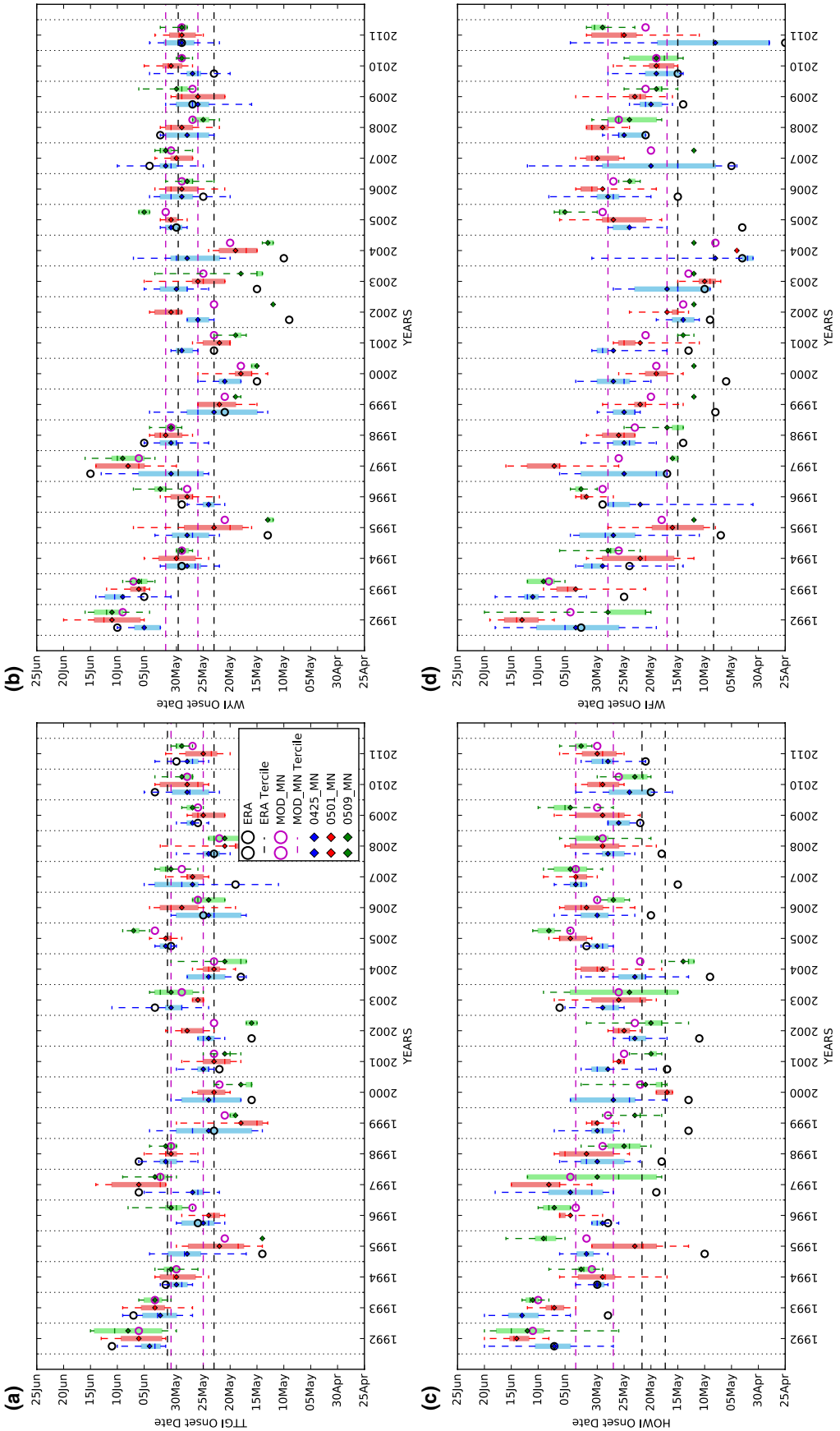

Fig. 2 Onset dates calculated from the monsoon onset indices with circles showing monsoon onset for MOD_MN (purple) and ERA-Interim (black). The diamonds show the ensemble onset date means of the three initializations, 0425 (blue), 0501 (red) and 0509 (green). The boxplots show the inter-ensemble spread of onset dates for different initializations, 0425 (light blue), 0501 (light red) and 0509 (light green). For each boxplot, whiskers show the range (max–min) of the onset dates, middle dash is the median and boxends show inter-quartile range of the inter-ensemble spread. The dashed horizontal lines show the upper and lower terciles for monsoon onset for MOD_MN (purple) and ERA-Interim (black). If the onset date of MOD_MN or ERA-Interim lies in between their respective upper and lower tercile lines, then it is considered a normal onset, but if it is before or after it is considered an early or late onset respectively. Monsoon onset dates for sub-figure are calculated with **a** TTGI, **b** WYI, **c** HOWI and **d** WFI

Table 2 Mean monsoon onset dates and their standard deviation (SD) for 20 years (1992–2011) with model ensemble members and ERA-Interim using the four different indices

	TTGI		WYI		HOWI		WFI	
	Mean	SD	Mean	SD	Mean	SD	Mean	SD
0425_ENS	28-May	3.4	29-May	4.1	30-May	4.9	23-May	7.8
0501_ENS	27-May	5.1	29-May	6.0	31-May	5.9	24-May	9.0
0509_ENS	27-May	7.1	26-May	9.1	30-May	8.5	21-May	8.9
MOD_ENS	28-May	6.8	28-May	8.0	31-May	8.3	23-May	10.8
ERA	27-May	8.1	26-May	10.0	21-May	8.4	13-May	9.3

Table 3 Monsoon onset date correlation for 20 years (1992–2011) for model means with respect to ERA-Interim using the four indices shown

	ERA			
	TTGI	WYI	HOWI	WFI
0425_MN	0.8*	0.6*	0.4	0.7*
0501_MN	0.7*	0.8*	0.5*	0.6*
0509_MN	0.9*	0.9*	0.6*	0.4*
MOD_MN	0.9*	0.9*	0.6*	0.7*

Values marked with an asterisk are statistically significant at the 95% confidence level

Table 4 Ratio of predictable component for each GloSea5 start-date initialization ensembles and model grand ensemble in predicting Indian monsoon onset date with respect to ERA-Interim using the four indices shown

	TTGI	WYI	HOWI	WFI
0425_ENS	1.3	0.9	0.6	1.0
0501_ENS	1.0	1.0	0.7	0.7
0509_ENS	0.9	1.0	0.6	0.5
MOD_ENS	1.3	1.2	0.9	1.0

3.2 WYI

The mean onset date using the large-scale circulation (vertical wind shear) index, WYI, with GloSea5 is 28 May which is close to ERA-Interim mean monsoon onset date (26 May) (Table 2). Interannual variability, measured by the standard deviation, shows that GloSea5 and ERA-Interim show similar variability (8 and 10 days respectively). Further, we note that GloSea5 performs very well in forecasting WYI onset dates for each year with an interannual correlation of 0.9 with ERA-Interim (Table 3). Johnson et al. (2017) and Kim et al. (2008) reported similar high correlations with reanalysis when considering interannual variability of the seasonal-mean WYI values for GloSea5, CFSv2, and ECMWF System 4 (0.66, 0.74 and 0.78 respectively). The RPC in GloSea5 for the WYI is very close to 1 for all initializations (Table 4), which reflects a close-to-perfect predictability potential. These results suggest that in modern dynamical seasonal forecast models, the large-scale monsoon circulation is well predicted. The large domain of WYI and the good representation of vertical wind shear in GloSea5 allows for the high correlation of WYI onset dates with reanalysis.

3.3 HOWI

The mean monsoon onset date calculated using HOWI for MOD_ENS is delayed compared to ERA-Interim by 10 days (Table 2), and the model ensemble spread for all three start dates is large (Fig. 2c). When considering interannual variability, the standard deviation of MOD_ENS and ERA-Interim is similar (8 days, Table 2). The interannual correlation between GloSea5 and ERA-Interim for HOWI (0.6, Table 3) is higher than that of the CMCC forecasting system compared to ERA-Interim (0.52) as described in Alessandri et al. (2015). The RPC with HOWI for GloSea5 is also lower than 1 for all start dates (Table 4), reflecting high signal-to-noise ratio. This suggests lower agreement with observations for ensemble means as the model might not be able to capture the signal.

The vertically integrated moisture flux, which is the basis of HOWI, is related to the zonal wind shear and moisture, and acts as an indicator of monsoon rainfall. Over the region of HOWI (Arabian Sea and southern India), the zonal wind and monsoon rainfall are very well correlated as grid-point anomaly correlations between the GloSea5 model mean and ERA-Interim and GPCP outputs respectively (Johnson et al. 2017, their Fig. 3). GloSea5 shows a climatological erroneous dry layer in the lower levels over the Arabian Sea and the Indian land surface extending to the mid-troposhere. Such a bias in the specific humidity, especially at the horizontal scale of the index, might lead to errors in the monsoon onset date defined using HOWI in GloSea5.

3.4 WFI

The mean onset date using the low-level zonal wind index, WFI, for MOD_ENS is delayed compared to ERA-Interim by 10 days (Table 2). In comparison to other modelling studies using a similar monsoon onset index called the onset circulation index (OCI; Wang et al. 2009), we note that CFSv1 shows a delayed mean onset date in comparison

with NCEP due to weak low-level winds (Saha et al. 2014). GloSea5 MOD_ENS and ERA-Interim onset dates standard deviations are close (10 and 9 days), similar to standard deviations of onset dates with NCEP and CFSv2 with the OCI index (Saha et al. 2014). The interannual correlation between ERA-Interim and GloSea5 MOD_MN with WFI is 0.7 (Table 3) and is similar to the correlation of OCI in the CMCC seasonal prediction system with ERA-Interim onset dates (0.65; Alessandri et al. 2015). On the other hand, according to Johnson et al. (2017), the correlation of seasonal-mean WFI values for GloSea5 with ERA-Interim is low (0.36), which led them to conclude that the local-scale monsoon circulation is not as well simulated in the model as the large scale. The RPC in GloSea5 MOD_ENS for WFI is also close to 1 but is lower for later start date initializations (Table 4). This reflects a high signal-to-noise ratio for the later start date initializations due to moderate agreement between the model and reanalysis. Our analysis in this section suggests that GloSea5 has high correlation with large-scale indices of monsoon onset (TTGI and WYI) compared to smaller scale indices (HOWI and WFI).

The correlation for hindcasts initialised from the latest start date (0509_MN) is lower with WFI. Monsoon onset dates estimated by WFI are usually earlier than the onset dates by other indices (Table 2). WFI represents the low-level shear vorticity over Indian monsoon trough (Wang et al. 2009), which is an early pre-cursor of the monsoon evolution, leading to earlier onset determination by this index relative to other indices. In our analysis, onset calculation defaults to day 1 if the onset index is already above the threshold at the start of the hindcast, but we cannot ignore those values. Thus, 0509_MN may not be able to accurately predict some early onsets dates with WFI and gives the first day in the time series (Figs. 2d; S1).

3.5 WLI

Moving on from the single-value monsoon onset indices, now we will discuss the WLI for local monsoon onset dates. We analyze mean local onset at each grid-point for each year (calculated from individual ensemble members onset dates) when compared against GPCP (Fig. 3). The mean monsoon onset pentad (1992–2011) in GloSea5 MOD_MN shows the earliest monsoon onset to occur over the Bay of Bengal and Arabian Sea similar to GPCP (Fig. S2), and the climatological monsoon onset dates calculated by Wang and LinHo (2002, their Fig. 6) using CMAP rainfall (1979–1998) and by Sperber et al. (2013; their Fig. 6) using GPCP rainfall

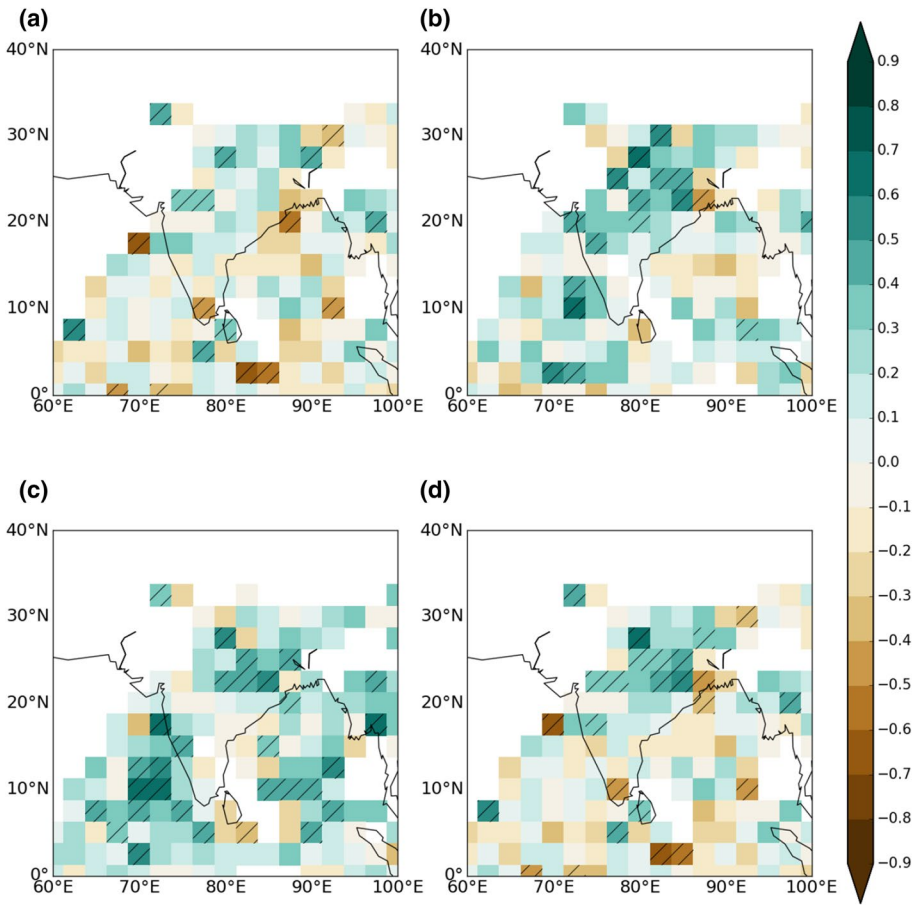

Fig. 3 Correlation of grid-point wise WLI onset pentads between **a** 0425_MN, **b** 0501_MN, **c** 0509_MN and **d** MOD_MN with respect to GPCP for 20 years (1992–2011). Stippling shows p-value less than 0.05 (significant at the 95% confidence level)

(1979–2007). However, the GloSea5 MOD_MN local monsoon onset over Bay of Bengal is not as early as in other studies, due to the limitations of the start dates of our hindcast. The GloSea5 hindcasts' overall monsoon progression, as understood from the spatial variation in monsoon onset pentads (Fig. S2), matches well with those of Wang and LinHo (2002, their Fig. 6). The monsoon onset over Kerala is between pentad 29–30 (Fig. S3a, b). The classical monsoon rainfall progression from south–east to north–west, perpendicular to the monsoon flow, starts from pentad 33 on the west coast of India and lasts until pentad 40 in northwestern India (Fig. S3k). Some parts of the leeward side of the Western Ghats mountains and Sri Lanka do not have relative precipitation exceeding 5 mm day^{-1} (Figs. S2; S3), similar to the observations in Wang and LinHo (2002, their Fig. 6), as these regions fall within the rain shadow. For detailed discussion on the local climatological monsoon onset progression in GloSea5 and associated physical mechanisms please refer to Menon et al. (2018).

The standard deviation of WLI monsoon onset pentads (1992–2011; Fig. S2) shows low interannual variation over central and northern-central India in observations. This was also found with another local agronomic monsoon onset index created by Moron and Robertson (2014; their Fig. 3b). Finally, we compared the interannual correlation of GloSea and ERA-Interim monsoon onset pentads calculated using WLI at each grid-point (Fig. 3). The monsoon onset interannual correlation over the southern Arabian Sea is positive in 0501_MN and 0501_MN. The 0425_MN correlation of onset dates with GPCP is low and has no significance (Fig. 3a). 0501_MN, 0509_MN and MOD_MN onsets have significant correlation with GPCP onset over parts of northern-central India (Fig. 3b–d; green stippling). From this discussion we note that it might be difficult to forecast the spatial pattern of the of the monsoon onset in any given year using a local-scale index such as WLI because the model may not be able to predict the local variations. But the monsoon onset forecast over regions with lower interannual variability (northern-central India) is much better and coincides with some of the major agricultural regions of India (Gangetic Plains).

4 Category-based monsoon onset forecast skill

In the previous section we noted that although the GloSea5 hindcasts are able to represent the interannual variations in monsoon onset with significant skill, the forecasting of the exact monsoon onset date is elusive. To better understand the predictability of the monsoon onset in GloSea5, we analyze the monsoon in terms of three tercile categories of early/normal/late onset (see Sect. 2.2.1 and Fig. 4). Detailed analysis of model skill in the remainder of this section will be based on monsoon onset tercile categories.

4.1 Monsoon onset tercile forecast skill in GloSea5

Monsoon onset forecast skill for model means has been compared against ERA-Interim in Fig. 5a, b for all single onset indices using ACC and HSS (see Sect. 2.2.2). The grand ensemble mean, MOD_MN, shows high accuracy at predicting WYI monsoon onset with ACC and HSS.

The overall performance of the individual model ensemble members (0425_ENS, 0501_ENS, 0509_ENS) in predicting early, normal or late onset is indicated by dBSS and dRPSS (see Sect. 2.2.2) shown in Fig. 5c–f. Higher positive values of these scores indicates better model skill (dRPSS and dBSS range from $-\infty$ to 1). Further, considering a climatological probability of occurrence of each tercile category as 1/3, value higher than 0 for dBSS and dRPSS is better than climatology. Thus, dRPSS and dBSS values of a forecasting system for tercile category of forecasts below 0 (demarcated in Fig. 5c–f as grey horizontal line) suggests a better forecast than climatology. dRPSS summarizes the model performance scores over the three tercile categories. In all cases the three start-dates have a dRPSS higher than 0, with model members performing best when WYI is used and performing worst with either WFI or HOWI. This could be due to fact that the model is able to simulate the large-scale circulation patterns well.

When considering the onset categories separately (using dBSS), we note that GloSea5 forecasts the late onset better than the early onsets. Previous studies show that late (early) onsets are associated with El Niño (La Niña) conditions (e.g. Xavier et al. 2007), as also observed in GloSea5 (detailed in the next section). ENSO conditions affect predictability of the monsoon onset, with indication of La Niña years having lower skill compared to El Niño years (Stolbova et al. 2016). Further, there is substantial asymmetry in the remote response to El Niño and La Niña conditions (Sardeshmukh et al. 2000), possibly leading to more skilful late onsets in GloSea5.

GloSea5 initialized at the longest lead times (0425 ensemble members) performs worse for late onsets all onset categories compared to other initializations, where as late initialization (0509 ensemble members) perform better at all the categories. Alessandri et al. (2015) also showed that the later initializations perform better than early initializations especially for late onsets. However, the prediction skill for tropical rainfall can change rapidly with ensemble size for small ensembles (Li et al. 2016) and that there might be a wide range of possible skill values from few random samples from a larger ensemble size, as in case for North Atlantic oscillation (Dunstone et al. 2016). This suggests that the small ensemble sizes of each start date, in our study, may

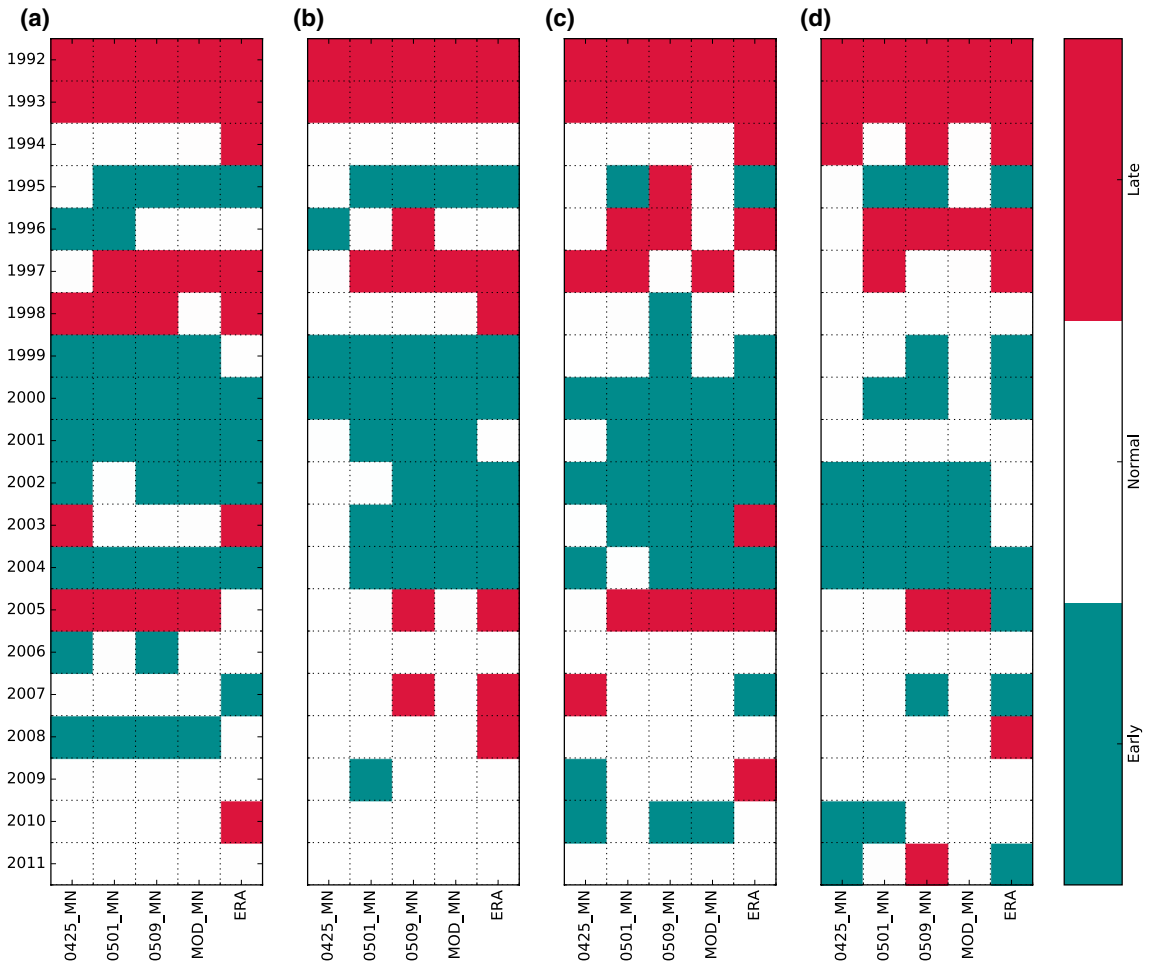

Fig. 4 Years with early, normal and late monsoon onset identified for MOD_MN and ERA-Interim with **a** TTGI, **b** WYI, **c** HOWI, **d** WFI

not allow the differences in skill between the start dates to be significant. However, the ensemble size correction term in our skill scores and the larger ensemble size of the grand ensemble (MOD_ENS) may allow for robust analysis of the skill in GloSea5 for predicting monsoon onset.

Model forecast skill analysis of onset tercile categories at each grid-point based on the WLI is shown in Fig. 6. Overall, GloSea5 has good skill over the Indian region (with ACC > 0.5 suggesting that $> 50\%$ of the forecasts are correct), with better performance over parts of northern-central India, central India, the Arabian Sea and Bay of Bengal, as also seen in MOD_MN and all three initializations (with positive HSS suggesting that the forecast skill is better than that of a random forecast).

4.2 The effect of ENSO forcing on monsoon onset forecast skill

To assess the possible improvement of forecasting skill under ENSO forcing in GloSea5 we compare forecast skill during the 11 identified ENSO years (ENSO11) against a distribution of forecast skill calculated from RANDOM11 (see Sect. 2.2.3). The RANDOM11 distributions for MOD_MN HSS skill-score for the four monsoon onset indices are shown in Fig. S4 as an example. To test the representation of the effect of ENSO forcing on monsoon onset forecast skill, we show the location of ENSO11 forecast skill-scores for MOD_MN (vertical lines). The position of the vertical line within the distribution is converted to a percentile rank score relative to the distribution. The higher the location (or percentile rank score) of the ENSO11 forecast skill-score within the distribution, the more confident we can be that ENSO is improving onset forecast prediction skill. Similarly, we calculate the percentile rank scores of ENSO11 derived from each start date ensemble mean against their RANDOM11 distributions for each index in Table 5.

In Table 5 when the percentile rank score exceeds 75%, then we can say with some confidence that there is improvement in onset forecast skill due to ENSO forcing, and we consider that percentiles lower than 25% show that

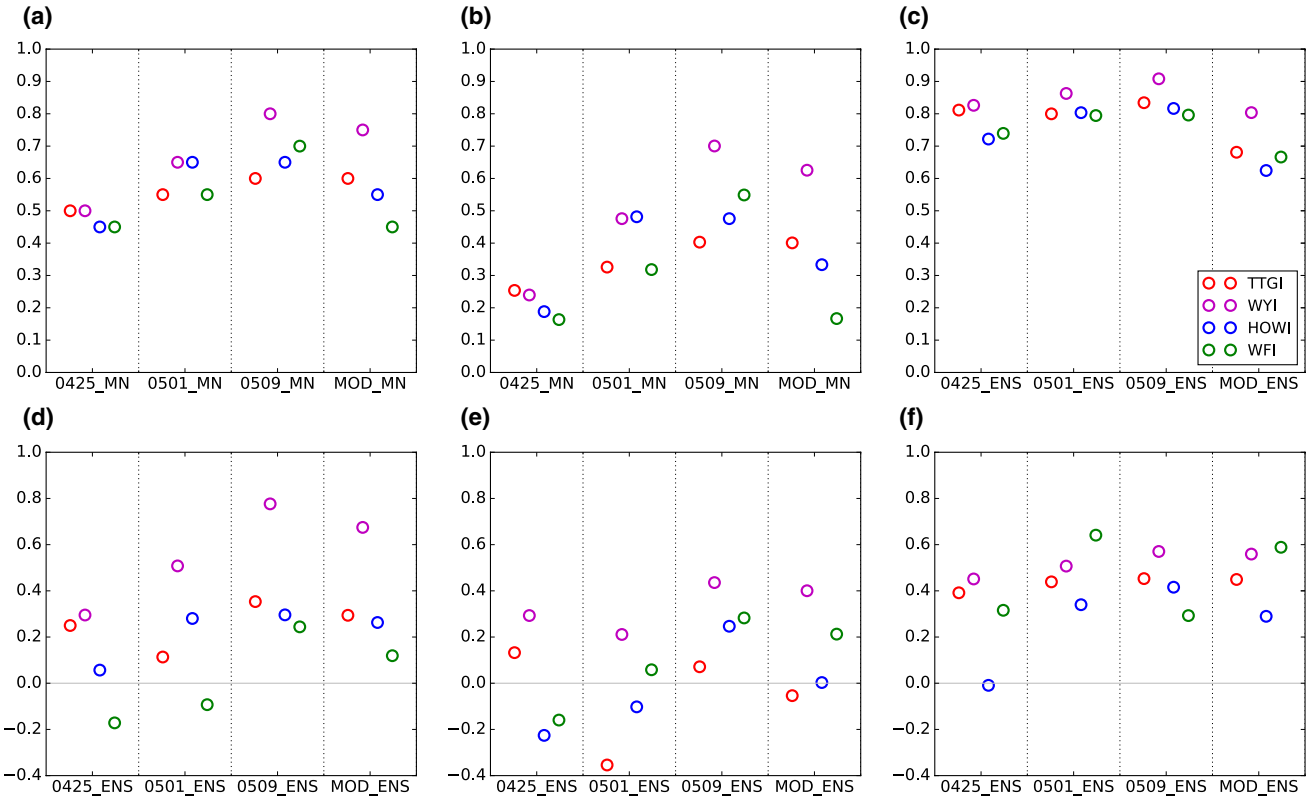

Fig. 5 Model skill-scores compared against ERA-Interim shown as **a** ACC, **b** HSS, **c** dRPSS, and dBSS of model for predicting **d** early onsets, **e** normal onsets and **f** late onsets. The colored circles show the skill calculated for model onset with the four different indices: WYI (magenta), WFI (green), TTGI (red), HOWI (blue). The grey horizontal line demarcates 0 threshold in **c**–**f**

skill is worse in ENSO years. We note that only in the case of WYI and TTGI monsoon onset with MOD_MN is any significant improvement observed in forecast skill for ENSO11 years. Whereas, forecast skill decreases in ENSO years when considering the HOWI monsoon onset index. Similar results are observed when considering individual start-date means. Improvement in monsoon onset forecast skill using large-scale circulation indices is reasonable considering the considerable evidence for ENSO affecting the vertical wind shear over India during monsoons (e.g. Webster and Yang 1992; Goswami and Xavier 2005). Further, similar improvement in the TTGI-based forecast skill is also observed during ENSO years, which could be due to the ENSO-related heating influencing the tropospheric temperature gradient over the southern Eurasia (Xavier et al. 2007). The decrease in HOWI onset forecast skill due to the inclusion of ENSO years can be explained by the low correlation between HOWI onsets and ENSO time-series as compared to other monsoon onset indices like TTGI (Moron and Robertson 2014). The study which defined this index also observed a low correlation between HOWI and ENSO, and suggested that there are years when the HOWI-ENSO relationship is not realized (Fasullo and Webster 2003).

With some evidence of the monsoon onset forecast skill improving in ENSO years, we move on to analyze the relationship between the tercile category of ENSO conditions (El Niño, ENSO-neutral and La Niña) and monsoon onset categories (early, normal and late). The frequency of occurrence of the nine different ENSO-onset combinations in GloSea5 are presented in Table 6. For this analysis we consider individual ENSO categories, with their respective three onset categories percentage frequencies as a probability distribution function (PDF). La Niña category has higher frequency of early onsets (except with WYI). However, the PDF is skewed away from late onset for all indices. Conversely, El Niño shows a strong shift in the PDF towards the late onsets with all indices. Neutral ENSO conditions have more frequent normal onsets, except with HOWI. This analysis shows that, similar to observational studies (Joseph et al. 1994; Xavier et al. 2007; Lau and Nath 2012; Adamson and Nash 2014), late monsoon onset in GloSea5 might be predisposed by developing El Niño conditions; neutral ENSO conditions tend to lead to normal onset and La Niña conditions predispose the monsoon to early onset in GloSea5. The results of Table 6 suggest that El Niño conditions increase the likelihood of late onsets, while La Niña conditions increase the likelihood of early onsets. Similar

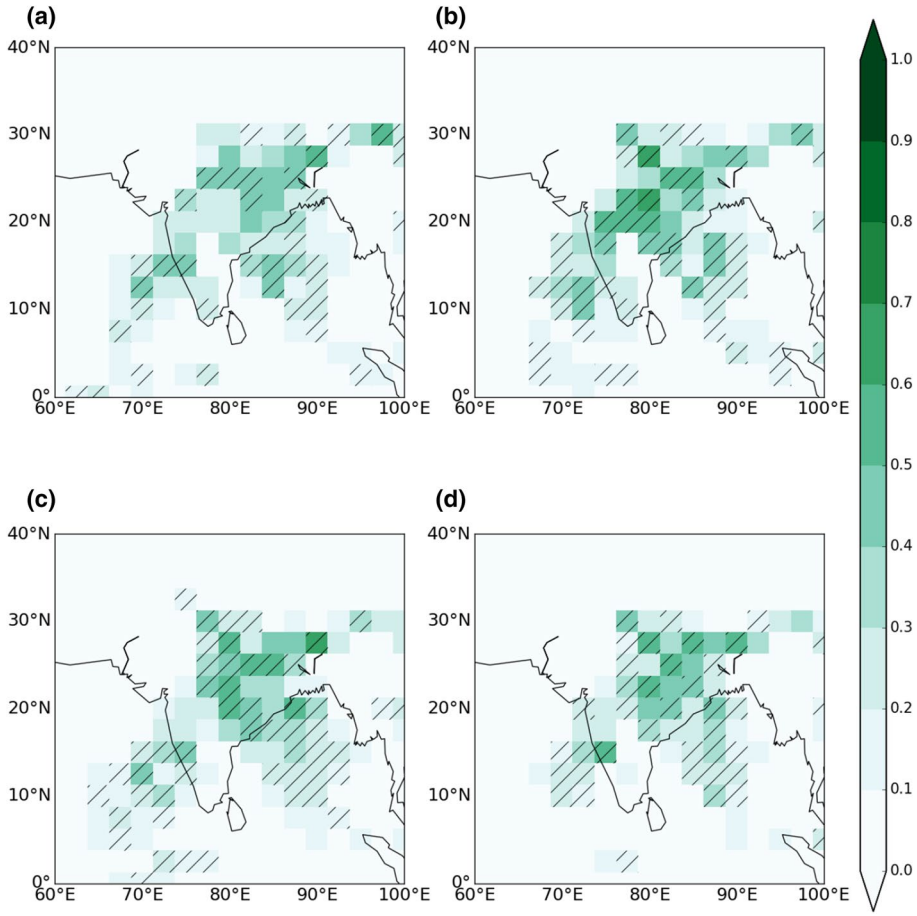

Fig. 6 ACC calculated at each grid-point for WLI onset pentads based on tercile categories for **a** 0425_MN, **b** 0501_MN, **c** 0509_MN and **d** MOD_MN with respect to GPCP for 20 years (1992–2011). The stippling shows regions of positive HSS

Table 5 Percentile rank score of the skill-score metrics (ACC and HSS) of GloSea5 ensemble means during ENSO11 for different monsoon onset indices skill-score distributions of RANDOM11

	ACC				HSS			
	0425_MN	0501_MN	0509_MN	MOD_MN	0425_MN	0501_MN	0509_MN	MOD_MN
TTGI	81.4	91.0	91.0	86.3	72.3	81.0	81.0	77.5
WYI	80.9	89.7	100.0	90.4	86.2	80.4	99.6	90.4
HOWI	34.4	27.8	5.8	8.2	20.5	20.7	2.3	5.8
WFI	35.2	90.9	100.0	69.4	23.8	82.2	99.2	53.2

to GloSea5, El Niño-like conditions influencing a delayed Indian monsoon onset is also seen in some CMIP3 models (Zhang et al. 2012) and the SINTEX-F2 coupled model (Prodhomme et al. 2015).

5 Summary and conclusions

We demonstrate the skill of the Met Office seasonal forecasting system, GloSea5-GC2, in predicting the interannual variability of the Indian monsoon onset using five different monsoon onset indices. GloSea5 simulates the climatological monsoon onset dynamics and thermodynamics well (Menon et al. 2018). In this study, using correlation analysis (with statistical significance testing) and various skill-scores, we show that GloSea5 can be used for forecasting Indian monsoon onset with modest-to-high skill one month in advance. When judged against indices computed from ERA-Interim reanalysis data, the monsoon onset prediction skill in GloSea5 is comparable or better than that shown in other contemporary coupled model forecast systems, despite similar or worse systematic biases. In GloSea5, large-scale monsoon features are better predicted than the local circulation and rainfall. Thus, when testing indices at small scales, GloSea5 shows only modest skill, but there is higher forecast skill with large-scale indices.

Despite modest skill in predicting the exact date of monsoon onset, GloSea5 has much better skill at forecasting the monsoon onset category based on terciles (early, normal or late). It represents early as well as late onsets

Table 6 Percentage frequency of each combination for onset categories (early, normal and late) during each ENSO condition (El Niño, neutral and La Niña) for all model ensemble members and start-date means from 1992–2011 for the four monsoon onset indices

Conditions		Percentage frequency			
ENSO	Onset	TTGI	WYI	HOWI	WFI
La Niña	Early	14.4	11.0	15.0	13.0
La Niña	Normal	11.3	13.0	13.6	13.0
La Niña	Late	7.3	9.0	4.5	7.1
Neutral	Early	9.9	14.4	9.9	11.9
Neutral	Normal	15.8	13.0	10.5	16.1
Neutral	Late	7.3	5.6	12.7	5.1
El Niño	Early	7.6	5.9	8.2	5.6
El Niño	Normal	8.2	9.6	9.9	8.8
El Niño	Late	18.1	18.4	15.8	19.5

Each column sums to 100%

better than a climatological forecast. The results of this hindcast study can be translated directly to the operational seasonal forecasting system. This study further suggests that GloSea5 will be able to predict early and late onsets well for operational forecasts with initializations of around one month lead time using these indices.

When considering the local grid-point onset pentads, GloSea5 perform well over parts of the core monsoon region (central India), the Gangetic plains (northern-central India) and coastal southern India. Better local monsoon onset forecasts over these regions are especially important for end-users due to the extensive agriculture practised there. The high skill of GloSea5 in forecasting interannual variations in monsoon onset is appreciable since the GloSea5 hindcast climatology shows only modest skill at simulating the interannual variations of summer mean (JJA) monsoon rainfall amount over India when compared against observed rainfall (Johnson et al. 2017).

While the assessment of Johnson et al. (2017) shows that Indian monsoon rainfall and circulation in GloSea5 may respond to ENSO forcing, our study suggests that only modest improvement is seen in monsoon onset predictability for years with ENSO forcing, and with WYI and TTGI indices for the grand ensemble mean. This may suggest that in GloSea5 both the major pathways of ENSO-Indian monsoon teleconnection (the changes in the vertical wind shear and the changes to the tropospheric temperature gradient over India) lead to ENSO forcing on the monsoon onset. Further, in GloSea5 different ENSO conditions are associated with a shift in the distribution of onset dates towards a tercile category. Results show El Niño years having a higher probability of a late monsoon onset and La Niña years have higher frequency of early monsoon onsets in GloSea5. A limitation of our study is the small number of study-years to significantly represent the ENSO-onset relationship.

In summary, this study presents GloSea5's suitability at predicting Indian monsoon onset dates using single-value large-scale indices. Its appreciable skill in predicting the local monsoon onset, over some agricultural regions of India, may be beneficial for using GloSea5 as a forecasting tool for end users such as farmers. There is very good skill in GloSea5 when predicting the tercile onset categories. Further analysis should address the link between dynamical, thermodynamical and hydrological monsoon indices and their impact on the interannual variability of monsoon onset prediction and its teleconnections, which may potentially improve seasonal forecasting of the Indian monsoon onset.

Acknowledgements The authors gratefully acknowledge the financial support given by the Earth System Science Organization, Ministry of Earth Sciences, Government of India (Grant no. MM/SERP/Univ_Reading_UK/2013/INT-13, manuscript number MM/TURNER/RP/03) to conduct this research under Monsoon Mission. In addition, the work was partly funded by INCOMPASS (NERC project NE/L01386X/1). S.J.W. was supported by the National Centre for Atmospheric Science, a NERC collaborative centre under the contract no. R8/H12/83/001/. G.M.M. and C.M. were supported by the Met Office Hadley Centre Climate Programme funded by BEIS and Defra. The authors would like to acknowledge the UK Met Office for providing their GloSea5-GC2 seasonal hindcast set. The ERA-Interim dataset used has been acquired from the ECMWF archive (http://apps.ecmwf.int/datasets/data/interim-full-daily). The GPCP dataset is provided by the ESRL: PSD archive (https://www.esrl.noaa.gov/psd/data/gridded/data.gpcp.html).

References

Adamson GC, Nash DJ (2014) Documentary reconstruction of monsoon rainfall variability over western India, 1781–1860. Clim Dyn 42(3–4):749–769

Adler RF, Huffman GJ, Chang A, Ferraro R, Xie PP, Janowiak J, Rudolf B, Schneider U, Curtis S, Bolvin D, Gruber A, Susskind J, Arkin P, Nelkin E (2003) The version-2 global precipitation climatology project (GPCP) monthly precipitation analysis (1979-present). J Clim 4:1147–1167

Alessandri A, Borrelli A, Cherchi A, Materia S, Navarra A, Lee JY, Wang B (2015) Prediction of Indian summer monsoon onset using dynamical subseasonal forecasts: effects of realistic initialization of the atmosphere. Mon Weather Rev 143(3):778–793

Ananthakrishnan R, Soman MK (1988) The onset of the southwest monsoon over Kerala: 1901–1980. J Climatol 8(3):283–296

Best MJ, Pryor M, Clark DB, Rooney GG, Essery RLH, Menard CB, Edwards JM, Hendry MA, Porson A, Gedney N, Mercado LM, Sitch S, Blyth E, Boucher O, Cox PM, Grimmond CSB, Harding RJ (2011) The Joint UK Land Environment Simulator (JULES),

model description part 1: energy and water fluxes. Geosci Model Dev 4:677–699. https://doi.org/10.5194/gmd-4-677-2011
Blockley EW, Martin MJ, Mclaren AJ, Ryan AG, Waters J, Lea DJ, Mirouze I, Peterson KA, Sellar A, Storkey D (2014) Recent development of the Met Office operational ocean forecasting system: an overview and assessment of the new Global FOAM forecasts. Geosci Model Dev 7:2613–2638. https://doi.org/10.5194/gmd-7-2613-2014
Bowler NE, Arribas A, Beare SE, Mylne KR, Shutts GJ (2009) The local ETKF and SKEB: upgrades to the MOGREPS short-range ensemble prediction system. Q J R Meteorol Soc 135:67–776
Dai A, Li H, Sun Y, Hong LC, Chou C, Zhou T (2013) The relative roles of upper and lower tropospheric thermal contrasts and tropical influences in driving Asian summer monsoons. J Geophys Res Atmos 118(13):7024–7045
Dee DP, Uppala SM, Simmons AJ, Berrisford P, Poli P, Kobayashi S, Andrae U, Balmaseda MA, Balsamo G, Bauer P, Bechtold P, Beljaars ACM, Berg LVD, Bidlot J, Bormann N, Delsol C, Dragani R, Fuentes M, Geer AJ, Dee DP (2011) The ERA-Interim reanalysis: configuration and performance of the data assimilation system. Q J R Meteorol Soc 137:553–597. https://doi.org/10.1002/qj.828
Dunstone N, Smith D, Scaife A, Hermanson L, Eade R, Robinson N, Andrews M, Knight J (2016) Skilful predictions of the winter North Atlantic oscillation one year ahead. Nat Geosci 9(11):809–815
Eade R, Smith D, Scaife A, Wallace E, Dunstone N, Hermanson L, Robinson N (2014) Do seasonal-to-decadal climate predictions underestimate the predictability of the real world? Geophys Res Lett 41(15):5620–5628
Fasullo J, Webster PJ (2003) A hydrological definition of Indian monsoon onset and withdrawal. J Clim 16(19):3200–3211
Findlater J (1969) A major lowlevel air current near the Indian Ocean during the northern summer. Q J R Meteorol Soc 95(404):362–380
Flatau MK, Flatau PJ, Rudnick D (2001) The dynamics of double monsoon onsets. J Clim 14:4130–4146
Flatau MK, Flatau PJ, Schmidt J, Kiladis GN (2003) Delayed onset of the 2002 Indian monsoon. Geophy Res Lett 30(14):1768
Gadgil S, RupaKumar K (2006) The Asian monsoon-agriculture and economy. In: Wang B (ed) The Asian monsoon. Springer, Berlin, pp 651–683
Goswami BN, Krishnamurthy V, Annmalai H (1999) A broadscale circulation index for the interannual variability of the Indian summer monsoon. Q J R Meteorol Soc 125(554):611–633
Goswami BN, Xavier PK (2005) ENSO control on the south Asian monsoon through the length of the rainy season. Geophys Res Lett 32:L18717
Goswami BN, Madhusoodanan MS, Neema CP, Sengupta D (2006) A physical mechanism for North Atlantic SST influence on the Indian summer monsoon. Geophys Res Lett 33(2):L02706
He H, Sui C-H, Jian M, Wen Z, Lan G (2003) The evolution of tropospheric temperature field and its relationship with the onset of Asian summer monsoon. J Meteorol Soc Jpn 81:1201–1223
Hsu HH, Terng CT, Chen CT (1999) Evolution of large-scale circulation and heating during the first transition of Asian summer monsoon. J Clim 12(3):793–810
Huffman GJ, Bolvin DT, Nelkin EJ, Wolff DB, Adler RF, Gu G, Hong Y, Bowman KP, Stocker EF (2007) The TRMM multisatellite precipitation analysis (TMPA): Quasi-global, multiyear, combined-sensor precipitation estimates at fine scales. J Hydrometeorol 8(1):38–55
IRI, The International Research Institute for Climate and Society (2013) Descriptions of the IRI climate forecast verification scores. http://iri.columbia.edu/wp-content/uploads/2013/07/scoredescriptions.pdf. Accessed on 9 Nov 2016
Johnson SJ, Turner A, Woolnough S, Martin G, MacLachlan C (2017) An assessment of Indian monsoon seasonal forecasts and mechanisms underlying monsoon interannual variability in the Met Office GloSea5-GC2 system. Clim Dyn 48(56):1447–1465
Joseph PV, Eischeid JK, Pyle RJ (1994) Interannual variability of the onset of the Indian summer monsoon and its association with atmospheric features, El Nino, and sea surface temperature anomalies. J Clim 7(1):81–105
Joseph PV, Sooraj KP, Rajan CK (2006) The summer monsoon onset process over South Asia and an objective method for the date of monsoon onset over Kerala. Int J Climatol 26(13):1871–1893
Kim HJ, Wang B, Ding Q (2008) The global monsoon variability simulated by CMIP3 coupled climate models. J Clim 21(20):5271–5294
Koteswaram P (1958) The easterly jet stream in the tropics. Tellus 10(1):43–57
Krishnamurthy V, Shukla J (2000) Intraseasonal and interannual variability of rainfall over India. J Clim 13(24):4366–4377
Lau NC, Nath MJ (2012) A model study of the air–sea interaction associated with the climatological aspects and interannual variability of the south Asian summer monsoon development. J Clim 25(3):839–857
Levine RC, Turner AG (2012) Dependence of Indian monsoon rainfall on moisture fluxes across the Arabian Sea and the impact of coupled model sea surface temperature biases. Clim Dyn 38(11–12):2167–2190
Li C, Yanai M (1996) The onset and interannual variability of the Asian summer monsoon in relation to land–sea thermal contrast. J Clim 9(2):358–375
Li C, Scaife AA, Lu R, Arribas A, Brookshaw A, Comer RE, Li J, MacLachlan C, Wu P (2016) Skillful seasonal prediction of Yangtze river valley summer rainfall. Env Res Lett 11(9):094002
MacLachlan C, Arribas A, Peterson KA, Maidens A, Fereday D, Scaife AA, Gordon M, Vellinga M, Williams A, Comer RE, Camp J, Xavier P, Madec G (2015) Global Seasonal forecast system version 5 (GloSea5): a high-resolution seasonal forecast system. Q J R Meteorol Soc 141(689):1072–1084. https://doi.org/10.1002/qj.2396
Megann A, Storkey D, Aksenov Y, Alderson S, Calvert D, Graham T, Hyder P, Siddorn J, Sinha B (2014) GO5.0: the joint NERC-Met Office NEMO global ocean model for use in coupled and forced applications. Geosci Model Dev 7:1069–1092
Menon A, Turner A, Martin G (2018) Modelling the moistening of the free troposphere during the northwestward progression of Indian monsoon onset. Q J R Meteorol Soc. https://doi.org/10.1002/qj.3281
Moron V, Robertson AW (2014) Interannual variability of Indian summer monsoon rainfall onset date at local-scale. Int J Climatol 34(4):1050–1061
Nanjundiah RS, Francis PA, Ved M, Gadgil S (2013) Predicting the extremes of Indian summer monsoon rainfall with coupled ocean-atmosphere models. Curr Sci 104(10):1380–1393
Murphy AH (1993) What is a good forecast? An essay on the nature of goodness in weather forecasting. Weather Forecast 8(2):281–293
Pai DS, Rajeevan MN (2009) Summer monsoon onset over Kerala: new definition and prediction. J Earth Syst Sci 118(2):123–135
Prakash S, Mitra AK, Momin IM, Rajagopal EN, Basu S, Collins M, Turner AG, Rao A, Ashok K (2015) Seasonal intercomparison of observational rainfall datasets over India during the southwest monsoon season. Int J Climatol 35(9):2326–2338
Parker DJ, Willetts P, Birch C, Turner AG, Marsham JH, Taylor CM, Kolusu S, Martin GM (2016) The interaction of moist convection and midlevel dry air in the advance of the onset of the Indian monsoon. Q J R Meteorol Soc 142(699):2256–2272
Prasad VS, Hayashi T (2005) Onset and withdrawal of Indian summer monsoon. Geophy Res Lett 32(20):1–4

Prodhomme C, Terray P, Masson S, Boschat G, Izumo T (2015) Oceanic factors controlling the Indian summer monsoon onset in a coupled model. Clim Dyn 44(3–4):977–1002

Rae JGL, Hewitt HT, Keen AJ, Ridley JK, West AE, Harris CM, Hunke EC, Walters DN (2015) Development of Global Sea Ice 5.0 and 6.0 CICE configurations for the Met Office global coupled model. Geosci Model Dev Discuss 8:2529–2554

Rajeevan M, Unnikrishnan CK, Preethi B (2012) Evaluation of the ENSEMBLES multi-model seasonal forecasts of Indian summer monsoon variability. Clim Dyn 38:2257–2274. https://doi.org/10.1007/s00382-011-1061-x

Rajeevan M, Nanjundiah RS (2009) Coupled model simulations of twentieth century climate of the Indian summer monsoon. In: Platinum jubilee special volume of the Indian Academy of Sciences, pp 537–568

Raju PVS, Mohanty UC, Bhatla R (2005) Onset characteristics of the southwest monsoon over India. Int J Climatol 25(2):167–182

Ramesh KJ, Basu S, Begum ZN (1996) Objective determination of onset, advancement and withdrawal of the summer monsoon using large-scale forecast fields of a global spectral model over India. Meteorol Atmos Phys 61(3):137–151

Rawlins F, Ballard SP, Bovis KJ, Clayton AM, Li D, Inverarity GW, Lorenc AC, Payne TJ (2007) The Met Office global fourdimensional variational data assimilation scheme. Q J R Meteorol Soc 133(623):347–362

Roy I, Tedeschi RG, Collins M (2016) ENSO teleconnections to the Indian summer monsoon in observations and models. Int J Climatol 37(4):1794–1813

Saha SK, Pokhrel S, Chaudhari HS, Dhakate A, Shewale S, Sabeerali CT, Salunke K, Hazra A, Mahapatra S, Rao AS (2014) Improved simulation of Indian summer monsoon in latest NCEP climate forecast system free run. Int J Climatol 34(5):1628–1641

Sardeshmukh PD, Compo GP, Penland C (2000) Changes of probability associated with El Nio. J Clim 13(24):4268–4286

Schneider E, Lindzen R (1976) On the influence of stable stratification on the thermally driven tropical boundary layer. J Atmos Sci 33:1301–1307

Senan R, Orsolini YJ, Weisheimer A, Vitart F, Balsamo G, Stockdale T, Dutra E, Doblas-Reyes FJ, Basang D (2016) Impact of springtime Himalayan–Tibetan Plateau snowpack on the onset of the Indian summer monsoon in coupled seasonal forecasts. Clim Dyn 47(9–10):2709–2725

Sperber KR, Annamalai H, Kang IS, Kitoh A, Moise A, Turner AG, Wang B, Zhou T (2013) The Asian summer monsoon: an intercomparison of CMIP5 vs. CMIP3 simulations of the late 20th century. Clim Dyn 41:2711–2744. https://doi.org/10.1007/s00382-012-1607-6

Soman MK, Kumar KK (1993) Space-time evolution of meteorological features associated with the onset of Indian summer monsoon. Mon Weather Rev 121(4):1177–1194

Stolbova V, Surovyatkina E, Bookhagen B, Kurths J (2016) Tipping elements of the Indian monsoon: prediction of onset and withdrawal. Geophy Res Lett 43(8):3982–3990

Syroka J, Toumi R (2004) On the withdrawal of the Indian summer monsoon. Q J R Meteorol Soc 130(598):989–1008

Taniguchi K, Koike T (2006) Comparison of definitions of Indian summer monsoon onset: better representation of rapid transitions of atmospheric conditions. Geophys Res Lett 33(2):1

Turner AG, Inness PM, Slingo JM (2005) The role of the basic state in the ENSO-monsoon relationship and implications for predictability. Q J R Meteorol Soc 131(607):781–804

Valcke S (2013) The OASIS3 coupler: a European climate modelling community software. Geosci Model Dev 6(2):373

Walters DN, Williams KD, Boutle IA, Bushell AC, Edwards JM, FieldPR Lock AP, Morcrette CJ, Stratton RA, Wilkinson JM, Willett MR, Brooks ME, Copsey D, Earnshaw PD, Harris CM, Manners JC, MacLachlanC Palmer MD, Roberts MJ, Tennant WJ (2017) The Met Office unified model global atmosphere 6.0/6.1 and JULES global land 6.0/6.1.0 congurations. Geosci Model Dev 10:1487–1520

Wang B, Fan Z (1999) Choice of South Asian summer monsoon indices. Bull Am Meteorol Soc 80(4):629–638

Wang B, Ding Q, Joseph PV (2009) Objective definition of the Indian summer monsoon onset. J Clim 22(12):3303–3316

Wang B, LinHo (2002) Rainy season of the Asian–Pacific summer monsoon. J Clim 15(4):386–398

Wang B, Wu R, Lau KM (2001) Interannual variability of the Asian summer monsoon: contrasts between the Indian and the western North Pacific–East Asian monsoons. J Clim 14(20):4073–4090

WCRP (2015) Forecast verification—issues, methods, and FAQ. http://www.cawcr.gov.au/projects/verification/. Accessed 1 Nov 2016

Weedon GP, Gomes S, Viterbo P, Shuttleworth WJ, Blyth E, H sterle, Adam JC, Bellouin N, Boucher O, Best M (2011) Creation of the WATCH forcing data and its use to assess global and regional reference crop evaporation over land during the twentieth century. J Hydrometeorol 12(5):823–848

Webster PJ, Yang S (1992) Monsoon and ENSO: selectively interactive systems. Q J R Meteorol Soc 118:877–926

Weigel AP, Liniger MA, Appenzeller C (2007) The discrete Brier and ranked probability skill scores. Mon Weather Rev 135(1):118–124

Williams KD, Harris CM, Camp J, Comer RE (2015) The Met Office global coupled model 2.0 (GC2) configuration. Geosci Model Dev 8(5):1509–1524. https://doi.org/10.5194/gmdd-8-521-2015

Xavier PK, Marzin C, Goswami BN (2007) An objective definition of the Indian summer monsoon season and a new perspective on the ENSO-monsoon relationship. Q J R Meteorol Soc 133(624):749–764

Yanai M, Li C, Song Z (1992) Seasonal heating of the Tibetan Plateau and its effects on the evolution of the Asian summer monsoon. J Meteorol Soc Jpn II 70(1B):319–351

Yatagai A, Kamiguchi K, Arakawa O, Hamada A, Yasutomi N, Kitoh A (2012) APHRODITE: constructing a long-term daily gridded precipitation dataset for Asia based on a dense network of rain gauges. Bull Am Meteorol Soc 93(9):1401–1415. https://doi.org/10.1175/BAMS-D-11-00122.1

Zeng X, Lu E (2004) Globally unified monsoon onset and retreat indexes. J Clim 17(11):2241–2248

Zhang Z, Chan JC, Ding Y (2004) Characteristics, evolution and mechanisms of the summer monsoon onset over Southeast Asia. Int J Climatol 24(12):1461–1482

Zhang H, Liang P, Moise A, Hanson L (2012) Diagnosing potential changes in Asian summer monsoon onset and duration in IPCC AR4 model simulations using moisture and wind indices. Clim Dyn 39(9–10):2465–2486